

DESIGN OF THE PEFP RCS*

J. H. Jang[#], H. J. Kwon, H. S. Kim, Y. S. Cho, PEFP/KAERI, Daejeon, Korea
Y. Y. Lee, BNL, Upton, New York 11973, U.S.A.

Abstract

As a feasible extension plan of the proton engineering frontier project (PEFP) 100-MeV proton linac, the conceptual design of a rapid cycling synchrotron (RCS) is under progress. The main purpose of the synchrotron is a spallation neutron source and it also includes the slow extraction option for basic and applied science research. In the initial stage, the beam power is 60 kW by using a scheme of 100-MeV injection and 1-GeV extraction. There is a scheme to increase power to 500 kW through a 3-stage upgrade. The injection and extraction energies will be 200-MeV and 2-GeV respectively after the final upgrade. This article summarizes the present status of the RCS design. It includes the physics design including injection and acceleration, and conceptual design of some magnets and RF cavity.

INTRODUCTION

Proton Engineering Frontier Project (PEFP) is the 100-MeV proton linac development project which was launched at 2002 and will be finished at 2012 [1]. As an extension plan of the linac, we are considering a rapid cycling synchrotron (RCS). The main purpose of the RCS is a spallation neutron source which can be used in the fields of the material science, bio technology, chemistry, etc.

As described in a physics design of the RCS [2,3], the basic design concepts of the PEFP RCS are as follows,

- The 100-MeV linac is the injector of the RCS.
- At the initial stage, the extraction energy is 1GeV and the beam power is 60 kW.
- The RCS should be upgradable in an injection energy, an extraction energy, and a repetition rate.
- The beam extraction methods includes both a fast extraction for the spallation neutron source and a slow extraction for the other purposes including medical research and RI production.
- The uncontrolled beam loss should be less than 1 W/m for hands-on maintenance.

The upgrade path of the RCS is summarized in Table 1. The beam power of the RCS is 60 kW in the initial stage and finally becomes 500 kW through the three-step upgrade. In the final stage, the injection energy is 200-MeV and the extraction energy is 2 GeV. This work summarized the lattice design and the beam dynamics study on the PEFP RCS. Table 2 summarizes the basic parameters of the RCS for this design study.

*Work supported by Ministry of Education, Science and Technology of the Korean government

[#]jangjh@kaeri.re.kr

Table 1: Upgrade plan of PEFP RCS

Stage	Injection Energy	Extraction Energy	Repetition Rate	Beam Power
Initial	100 MeV	1 GeV	15 Hz	60 kW
1	100 MeV	1 GeV	30 Hz	120 kW
2	100 MeV	2 GeV	30 Hz	250 kW
3	200 MeV	2 GeV	30 Hz	500 kW

Table 2: Design parameters PEFP RCS in the initial stage.

Injected Particle	H-
Lattice Structure	FODO
Super-period	4
Number of Cell	20
Number of Dipoles	32
Machine Tune [Qx /Qy]	4.39 / 4.29
Transition γ	4.4
Circumference [m]	224.16
RF Harmonic	2
RF Voltage	75 kV

PEFP RCS DESIGN

The PEFP RCS has a four-fold symmetry in order to reduce the lower order resonance. The basic lattice is a regular FODO structure and one super-period includes five FODO cells. The lattice structure of the RCS was given in Figure 1. The four dispersion-free straight sections are reserved for injection and extraction, RF cavities and beam collimation. The arc straight sections can be used for the momentum collimation and slow extraction. The lattice functions are given in Figure 2 [2].

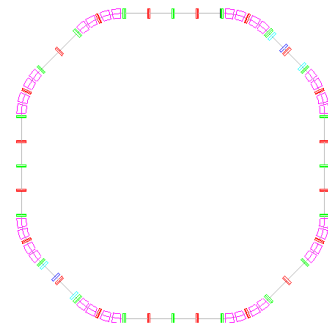


Figure 1: PEFP RCS lattice.

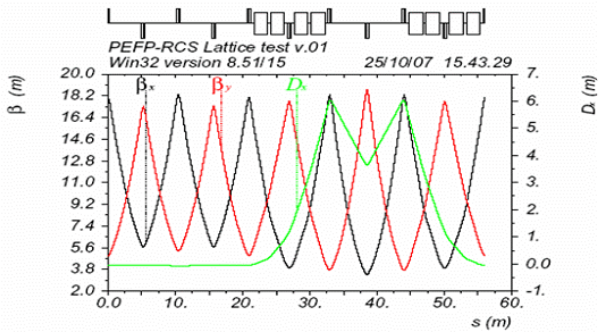


Figure 2: Beta functions and dispersion function in a super-period of the PEFP RCS

The RF harmonic is two in this RCS and there are two bunches in a synchrotron pulse [4]. The linac beam has to be chopped in order to reduce beam losses in the capture and acceleration process. In the 15-Hz operation, one macro-pulse of linac beams includes 400 mid-pulses with the pulse width of 500 ns. It corresponds to the chopping factor of 57%. In the RCS, there are two bunches in a pulse. After a injection period, 200 linac pulses are injected into each RF bucket. The proton number in a synchrotron pulse is 2.5×10^{13} . The time structure of the linac and RCS beams is given in Figure 3.

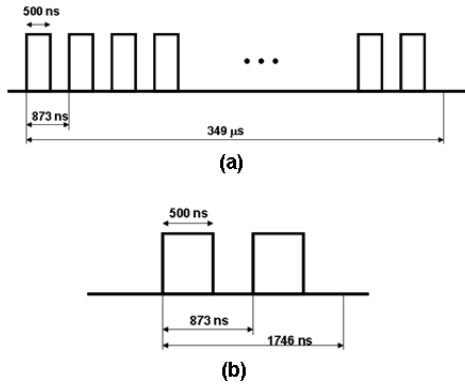


Figure 3: Time structure of (a) mid-pulses in a macro-pulse of linac beams and (b) bunches in a pulse of the RCS beams.

The injection of the PEFP RCS is based on H^- charge exchange injection with a transverse painting method [3, 5]. The injection system consists of a chicane magnet which deforms the horizontal DC orbit up to 105 mm and the four ferrite cored magnets which are used for the fast change of the painting bump in the horizontal and vertical directions. The overall scheme of RCS injection is illustrated in Figure 4 [3]. The particle distributions in x-y, x-x' and y-y' spaces after finishing injection with a correlated painting are given in Figure 4. In this simulation we used ORBIT code [6] with 40,000 macro particles [3].

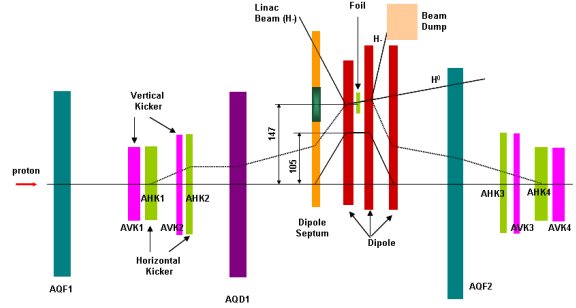


Figure 4: Layout of the injection system for PEFP RCS.

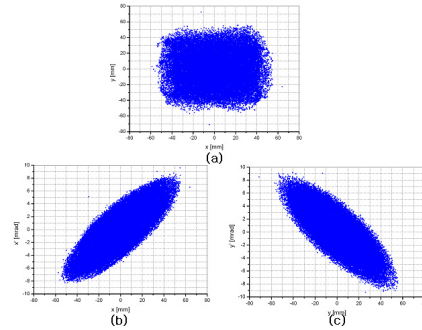


Figure 5: Particle distribution after injection with correlated painting in (a)x-y space, (b) x-x' space, and (c) y-y' space.

We also studied the dynamic aperture of the PEFP RCS in the initial operation [7]. The main focuses are the effects of the fractional momentum spread, magnet misalignment, magnet amplitude errors and magnet multipole components of dipole magnets. For the simulation, we used the DYNAP routine in MAD8 [8]. Because the maximum value of the fractional momentum deviation is 0.7 % in the injection and acceleration simulation [4], we studied its effects on the dynamic aperture by varying from 0.0% to $\pm 0.7\%$. Figure 6 shows the dynamics aperture depending on the fractional momentum deviation. The blue curve describes the stable beam region which is given by $\sqrt{\frac{2\beta\epsilon}{\pi}} + \eta \frac{\delta p}{p} + cod$ where β and ϵ represent the

beta function and beam emittance. The parameter η is the dispersion function of the ring. The cod represents the closed orbit distortion which is less than 1 mm after the orbit correction. This closed orbit distortion effects on the dynamic aperture is given in Figure 7. We assumed that the displacement and rotation errors of the magnets are less than 300 μm and 1 mrad, respectively, and the magnet field errors are less than 10^{-4} . Each quadrupole magnet has a corrector magnet. We found the dynamic aperture moves to outside (red line) of the stable region after the orbit correction even though it is inside (black line) before correction. Finally we studied the dynamic aperture variation by the multi-pole components of the bending magnet. The errors include quadrupole, sextupole, and octupoles which are assumed to be less than 10^{-4} of

the dipole amplitude. We found that the effects can be negligible.

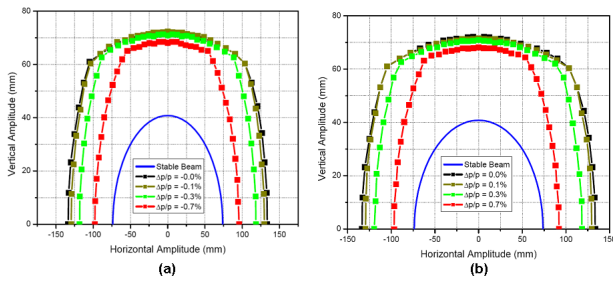


Figure 6: Fractional momentum deviation and dynamic aperture in the LIE algebra tracking method: (a) $0 \sim -0.7\%$, (b) $0 \sim 0.7\%$.

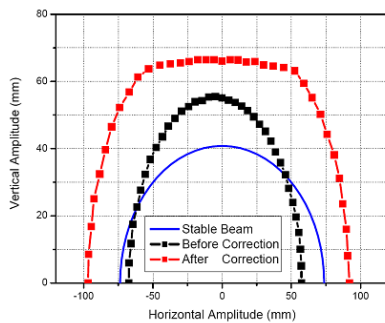


Figure 7: Orbit distortion and dynamic aperture: black line before correction and red line after correction.

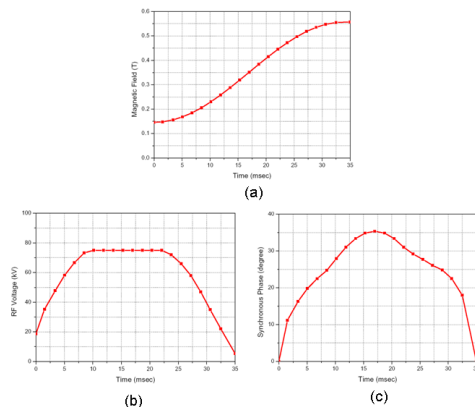


Figure 8: Ramping of (a) magnetic field, (b) RF voltage and (c) the synchronous phase.

Next we performed the acceleration simulation in order to study the magnet and RF ramping for the large capture rate [3, 4]. In this study we used a sinusoidal ramping of the magnetic field (Figure 8). The RF voltage program and the corresponding synchronous phase variation are given in Figure 8. The initial RF voltage is 18.7 kV and the maximum voltage is 75.0 kV. The synchronous phase increases up to about 35 degrees. We used the RAMA program to get the initial ramping of the RF voltage [9].

Figure 9(a) shows the particle distribution in the longitudinal phase space just after injection. We found that there is no beam loss up to 200 injection turns. The particle distribution is given in Figure 9(b) for 1 GeV beams. The final energy and capture rate are 1.003 GeV and 99.91%, respectively. The most beam loss happens in the initial ramping stage [3, 4].

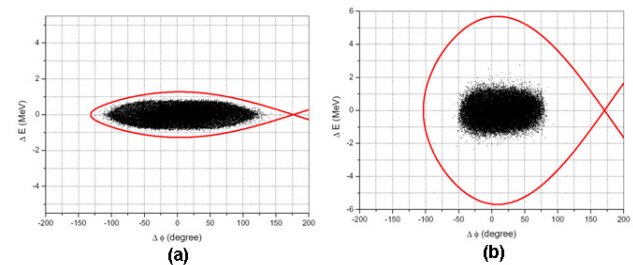


Figure 9: Particle distribution in the RF bucket: (a) just after injection and (b) after full acceleration for 1 GeV.

CONCLUSION

This work summarized the results on the lattice design and the beam dynamics study of the PEFP RCS in the initial stage where the beam power is 60 kW with a 15-Hz operation. The injection and extraction energies are 100 MeV and 1 GeV, respectively.

REFERENCES

- [1] J. Jang, Y. Cho, B. Choi, J. Kim, K. Kim, J. Park, "The Korean Proton Engineering Frontier Project", HB 2008, Nashville, August 2008.
- [2] B. Chung, Y. S. Cho, Y. Y. Lee, "Conceptual Design of the PEFP Rapid Cycling Synchrotron", PAC'07, Albuquerque, June 2007, THPMN046, p. 2817 (2007); <http://www.JACoW.org>.
- [3] J. H. Jang, H. J. Kwon, Y. S. Cho, Y. Y. Lee, "Physics Design of the PEFP RCS", PAC'09, Vancouver, Canada, May 2009.
- [4] J. H. Jang, H. J. Kwon, Y. S. Cho, Y. Y. Lee, "Acceleration Simulation of PEFP RCS for a 1-GeV Extraction", Korean Nuclear Society Spring Meeting, 2009.
- [5] J. H. Jang, Y. S. Cho, Y. Y. Lee, "Injection Simulation Result of the PEFP RCS", Korean Physical Society Autumn Meeting, 2008.
- [6] J. Galambos, J. Holmes, D. Olsen, A. Luccio, J. Beebe-Wang, "ORBIT User Manual", 1999.
- [7] J. H. Jang, Y. S. Cho, H. J. Kwon, H. S. Kim, "Dynamic Aperture of PEFP RCS", Korean Nuclear Society Autumn Meeting, 2009.
- [8] H. Grote and F. C. Iselin, "The MAD Program: Users Reference Manual", Version 8.19, CERN/SL/90-13.
- [9] R. Baartman, H. Schonauer, "RAMA: A Computer Code Useful for Designing Synchrotrons", TRI-DN-86-15, 1986.